Pulsed-laser deposition and laser-induced breakdown spectroscopy of functional oxide materials

Johannes D. Pedarnig * [a, b]
[a] Institute of Applied Physics, Johannes Kepler University, A-4040 Linz, Austria
[b] Christian Doppler Laboratory for Laser – Assisted Diagnostics,
Johannes Kepler University, A-4040 Linz, Austria

ABSTRACT

Pulsed-laser deposition (PLD) and laser-induced breakdown spectroscopy (LIBS) techniques are reviewed and new results on PLD and LIBS of functional oxide materials are reported. Nano-composite high-T_c superconducting (HTS) films with enhanced critical current density are produced by laser ablation of novel ceramic targets. The transport properties of HTS thin films are modified by light-ion irradiation. Nano-patterning of HTS films is achieved by masked ion beam irradiation. Optically transparent epitaxial ZnO layers are grown by PLD and acoustic resonances in the GHz range are excited by piezoelectric actuation. LIBS is employed to analyze impurity trace elements in industrial oxide powder. For quantitative analysis of major and minor elements the calibration-free LIBS method is refined. This CF-LIBS method is employed to the analysis of multi-element materials and very good match with nominal concentration of oxides is achieved (relative error less than 20 %).

Keywords: Pulsed-laser deposition, laser-induced breakdown spectroscopy, calibration free laser-induced breakdown spectroscopy, thin films, functional oxides, multi-component materials

1. INTRODUCTION

Pulsed-laser deposition (PLD) and laser-induced breakdown spectroscopy (LIBS) are techniques used for materials synthesis and analysis that are based on the ablation of material by means of short and intense pulses of laser radiation. In PLD, some part of the laser ablated material is condensed on a substrate[1-3]. The condensed species can nucleate at the substrate surface forming thin films, multi-layer structures, and various kinds of nano-structures depending on the type of material and the experimental parameters employed. Different classes of material including oxides, nitrides, oxy-nitrides, borides, metals, polymers, semiconductors, nano-composite materials and novel materials like iron arsenide pnictides can be grown as thin films by PLD. In LIBS, the optical emission of the laser-induced plasma is collected and analyzed using sensitive spectrometers and detectors[4-8]. From the measured LIBS spectrum the type and concentration of emitting species in the plasma (elements and molecules) can be determined. This method offers multi-elemental detection capability and is used in fundamental research, e.g. as complementary analysis tool, and for technical applications, e.g. for in-situ and remote monitoring in industrial processes. LIBS can be employed to solid, liquid, and gaseous materials, and also to dispersed materials such as colloidal suspensions and biological, organic, and inorganic aerosols.

In PLD and LIBS nano-second laser pulses are employed for the ablation of target material, typically. Solid-state lasers (e.g., Nd:YAG, fundamental wavelength $\lambda = 1064$ nm, higher harmonics at $\lambda = 532$ nm, 355 nm, 256 nm), excimer lasers (e.g., ArF, $\lambda = 193$ nm; KrF, $\lambda = 248$ nm), and UV gas lasers (e.g., F_2, $\lambda = 157$ nm) with pulse lengths $\tau \approx 5 - 25$ ns are frequently used. The pulsed radiation is focused onto the target materials and the laser fluence in the spot is several J/cm^2, typically. Thin film deposition is performed in a PLD chamber in controlled inert or reactive gas background at pressure $p \leq 1$ mbar. Epitaxial films are grown on lattice-matched and chemically compatible substrate crystals that are heated during deposition. LIBS measurements are performed in gas or liquid background. Frequently, measurements are done in air or in nitrogen (N_2) and argon (Ar) gas atmosphere. The optical emission of laser-induced plasma is analyzed by gated spectrometers and sensitive photo detectors.

*Johannes.Pedarnig@jku.at; phone 0043 732 2468 9246; fax 0043 732 2468 9242; www.applphys.jku.at

17th Slovak-Czech-Polish Optical Conference on Wave and Quantum Aspects of Contemporary Optics,
edited by Jarmila Müllerová, Dagmar Senderáková, Stanislav Jurecka, Proc. of SPIE
Vol. 7746, 774607 · © 2010 SPIE · CCC code: 0277-786X/10/$18 · doi: 10.1117/12.881430

2. PULSED-LASER DEPOSITION OF FUNCTIONAL OXIDE MATERIALS

Figure 1 shows the basic experimental setup of a PLD system[1]. The laser radiation is focused onto the surface of solid or liquid targets and the laser-induced plasma plume is expanding strongly forward directed and perpendicular to the irradiated spot on the target. The substrates that are heated from the backside typically. Target and substrate are usually placed with their surfaces oriented parallel to each other (so-called "on-axis" geometry). The distance between target and substrate is several cm depending on the deposition parameters employed. In "off-axis" geometry the substrate is placed perpendicular to the target.

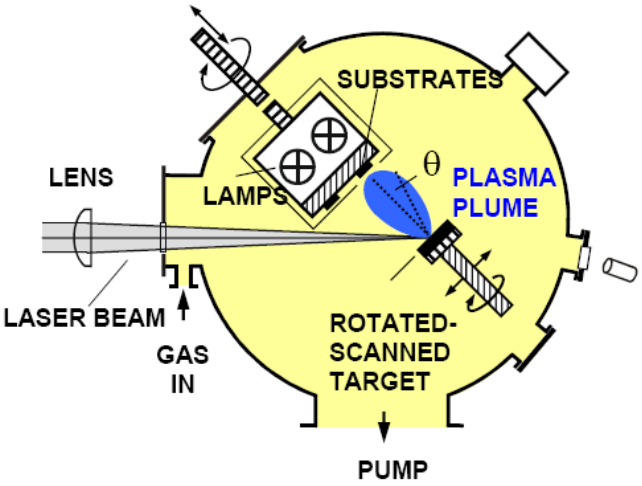

Figure 1. Schematic of experimental setup for pulsed-laser deposition of thin films in "on-axis" geometry. The distance between target and substrate is several cm, typically.

Many variants of PLD are described in the literature, for example, dual-beam ablation with colliding plasma, gas-pulse supported deposition, plasma-assisted deposition, deposition on inclined (or off-axis) substrates, electron-beam or ion-beam assisted deposition, magnetic plume guiding, etc[1-3].

In PLD, the through-put in terms of coated substrate area or amount of deposited material per time unit is usually small. The through-put is limited mainly by the small size of substrates (few cm^2, typically) and the low laser pulse repetition rate (≤ 20 Hz, typically). The deposition rate in PLD of high-temperature superconducting $YBa_2Cu_3O_7$ (YBCO) thin films on MgO substrate crystals (size 1 cm^2) is around 0.1 nm × m^2 / h, for example. High-throughput fabrication of PLD films requires high repetition rate lasers (e.g., 300 Hz, pulse energy 1 J, 248 nm KrF), suitable deposition geometry for large-area "substrates" (e.g., reel-to-reel "R-2-R" systems for coating of long-length substrate tapes), novel heater designs, and an efficient utilization of target material (e.g., by using multiple plasma plumes, etc). Examples for high-throughput PLD include the fabrication of YBCO films on 100 m long tapes at a deposition rate of about 40 nm × m^2 / h [reference 9, and references therein] and the deposition of GdBCO coated conductors on 500 m long metal tapes in an R-2-R process[10]. Another limitation in PLD is the formation of particulates on film surfaces[1]. Mechanisms of particulate formation include vapor phase condensation, the ejection of melt droplets and larger fragments from targets, the growth of secondary phases in films, and off-stoichiometric deposition. The optimization of PLD parameters such as laser fluence, background pressure, and target scanning (translation, rotation) enables to reduce the coverage of films by particulates. Furthermore, different in-situ and ex-situ techniques can be employed to avoid the formation of larger particulates and to remove such particulates from deposited films, respectively. In-situ techniques are employed during PLD and include the use of gated mechanical shutters and shadow masks (eclipse method), the deposition on off-axis placed substrates, and the ablation from two targets producing overlapping plasma (crossed beam

PLD). Methods employed for the removal of particulates after film deposition (ex-situ) are based on ion beam processing (milling) and chemical-mechanical polishing (CMP).

Oxide materials reveal a plethora of dielectric, electric, magnetic, and (multi)ferroic phenomena[11]. Thin films of functional oxide materials have a high potential for device applications, for example in future electric field-effect devices, superconducting Josephson junctions, magnetic tunnel junctions, and high-frequency devices. Table 1 summarizes some important functional oxide materials and potential applications of oxide thin films.

Table 1. Examples of functional oxide materials and thin film applications.

PHYSICAL PROPERTY OF OXIDES		THIN FILM APPLICATION
Ferroelectric	$PbZr_xTi_{1-x}O_3$, $BaTiO_3$	Data storage: non-volatile Fe-RAM
Piezoelectric	ZnO , $PbZr_xTi_{1-x}O_3$	Sensors, actuators
Magnetic, magnetoresistive	$La_xA_{1-x}MnO_3$ (A = Ba, Sr, Ca), Fe_3O_4 , Sr_2FeMoO_6	Data storage: non-volatile M-RAM, Spintronics
Doped dielectric	(Co, Fe):TiO_2 , $Nd_xSr_{1-x}MnO_3$	High-T_c ferromagnetic devices, Electric field effect devices
High-T_c superconductive	$YBa_2Cu_3O_{7-d}$	Coated conductors, Josephson junction devices
Wide band-gap semiconducting	ZnO , $Zn_xMg_{1-x}O$	Transparent conductive oxide, UV photonics
Electro-optic	$LiNbO_3$	Photonics, optoelectronics
Optically active	RE-doped Y_2O_3, Al_2O_3	Integrated optics
Electro-chemical	$La_{1-x}Sr_xCoO_3$	Solid oxide fuel cells
Thermo-electric	$NaCo_2O_4$, $Ca_3Co_4O_9$	Microelectronic cooler
Bio-active	$Ca_{10}(PO_4)_6(OH)_2)$, TiO_2	Anti-bacterial coatings
Multi-ferroic	$BiFeO_3$	Novel ferro-electro-magnetic devices
High- k dielectric	HfO_2 , ZrO_2 , $LaAlO_3$, YSZ	Novel gate dielectrics (MOSFETs)

Interfaces and multi-layers of oxide materials can show additional phenomena as, for example, the formation of a quasi two-dimensional electron gas at the interface of insulating oxides[12, 13], the correlation of defects and pinning centers in high-temperature superconducting (HTS) cuprates[14], and the enhanced polarization in asymmetric ferroelectrics[15]. The fabrication of such oxide films and multi-layers requires precise control of growth conditions. Atomically sharp interfaces can be produced by characterizing growing films in-situ using electron beam diffraction and ion scattering techniques (e.g., RHEED and TOF-ISARS, respectively). PLD also allows producing non-planar micro-structures and nano-structures, for example ZnO based quantum well heterostructures on vertical ZnO nano-wires[16]. In our group we have grown various types of oxide thin films, multi-layers, and nano-composite layers recently. The thin film materials include high-T_c superconductors like $YBa_2Cu_3O_7$ (YBCO) [17], $Bi_2Sr_2Ca_{n-1}Cu_nO_{2(n+2)+\delta}$ [18], and $HgBa_2Ca_{n-1}Cu_nO_{2n+2+\delta}$ [19], piezoelectrics based on ZnO [20, 21], and glass doped with rare earth elements[22]. Nano-composite HTS layers based on YBCO yield enhanced critical current density[23].

The transport properties (temperature dependent resistivity) and the critical temperature T_c of HTS thin films are modified by low-energy light-ion irradiation[24]. The irradiation of YBCO films by 75 keV He^+ ions generates point defects in the HTS materials without destruction of the YBCO unit cell lattice structure (ion dose $\leq 5 \times 10^{15}$ ions / cm^2). The room temperature resistivity measured in situ during ion irradiation increases approximately exponentially with employed ion dose[25]. This behavior can be described tentatively with a simple resistor network model. The model

assumes a modification of transport properties in some region of the film due to collisions of an incident He^+ ion with target ions[25]. Further collisional events in the same film region due to subsequent He^+ ion impact are neglected. The T_c (defined at half-transition) is rapidly suppressed with increasing ion dose. A dose of 3×10^{15} ions/cm^2 marks the crossover from superconducting material with metallic-like temperature dependence to a semiconducting temperature behavior and the disappearance of superconductivity. Relaxation processes and photo-induced changes of transport properties of He^+ ion-irradiated YBCO films are studied in reference[26].

Ion irradiation through appropriate stencil masks allows for large-area micro-patterning and nano-patterning of films in a direct and single-step process without etching of film material. Figure 2 shows scanning electron microscopy (SEM) images of YBCO thin films patterned by masked ion beam structuring (MIBS). Prior to ion irradiation the PLD films were surface-planarized by CMP treatment[27].

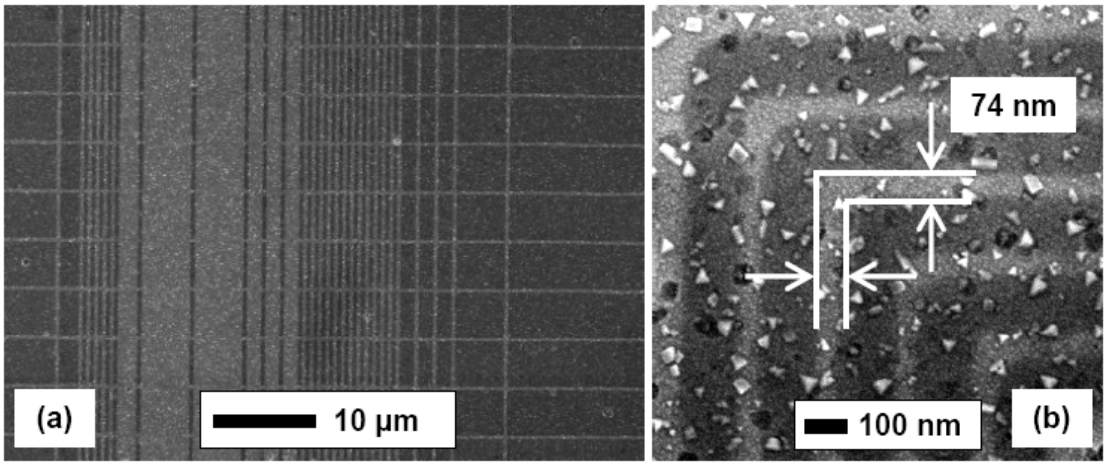

Figure 2. SEM images of YBCO thin film surfaces patterned by masked ion beam structuring. Ion irradiated regions of films appear relatively darker, non-irradiated YBCO film regions are brighter. Irradiated micro-structures (a) and nano-structures (b). Solid white lines are guides to the eye (b).

Regions irradiated by He^+ ions (75 keV energy, ion dose 3×10^{15} ions/cm^2) appear darker in SEM imaging using secondary electron detection. Various film structures can be patterned depending on the structure of stencil masks used. Stripe pattern with line-to-line spacings of less than 100 nm are easily irradiated (b).

3. LASER-INDUCED BREAKDOWN SPECTROSCOPY OF FUNCTIONAL OXIDE MATERIALS

The LIBS method is employed in various fields including materials identification, environmental monitoring, detection of hazardous materials, and for different on-site and in-line industrial applications[28, 29]. In LIBS, the limit of detection (LOD) for trace impurity elements is few ppm, typically, depending on the element and the matrix material. The detection sensitivity is limited mainly by the transient nature of the laser-induced plasma, the small amount of sampled material, the relatively low plasma temperature, and the ejection of non-luminous particles from laser-irradiated targets. We have analyzed different types of oxide materials by LIBS including industrial iron oxide nano-powder[30] and superconducting copper-oxides doped with secondary oxide phases[31].

The quantitative element analysis and determination of oxide concentration in multi-component materials is an important task in LIBS and is relevant in various fields of applications (e.g.: analysis of ores, concrete, slag). Calibration free laser-induced breakdown spectroscopy (CF-LIBS) and the multivariate calibration are among the methods employed for quantitative concentration analysis of complex materials. The CF-LIBS method has been introduced recently[32]. We developed a modified CF-LIBS algorithm in order to increase the accuracy of element and oxide concentration values

calculated from measured LIBS spectra[33]. This algorithm includes a fast iterative correction of radiation self-absorption effects and of plasma parameters. For testing of the algorithm, mixed oxide pellets containing different amount of Fe_2O_3, MgO, and CaO material were prepared and analyzed. Table 2 shows the oxide concentration for five different samples produced by mixing of appropriate amount of oxide powders and by hydraulic pressing of powder mixtures into pellets.

Table 2. Nominal oxide concentration of samples analyzed by CF-LIBS.

Concentration [wt %]	**Sample #**				
	1	**2**	**3**	**4**	**5**
Fe_2O_3	33.33	38.53	16.71	24.98	9.76
MgO	33.33	7.61	24.99	8.33	9.04
CaO	33.33	53.86	58.30	66.69	81.20

LIBS spectra were measured for different delay times and spectra were de-convolved with the instrument function. Appropriate emission lines were selected for the CF-LIBS analysis.

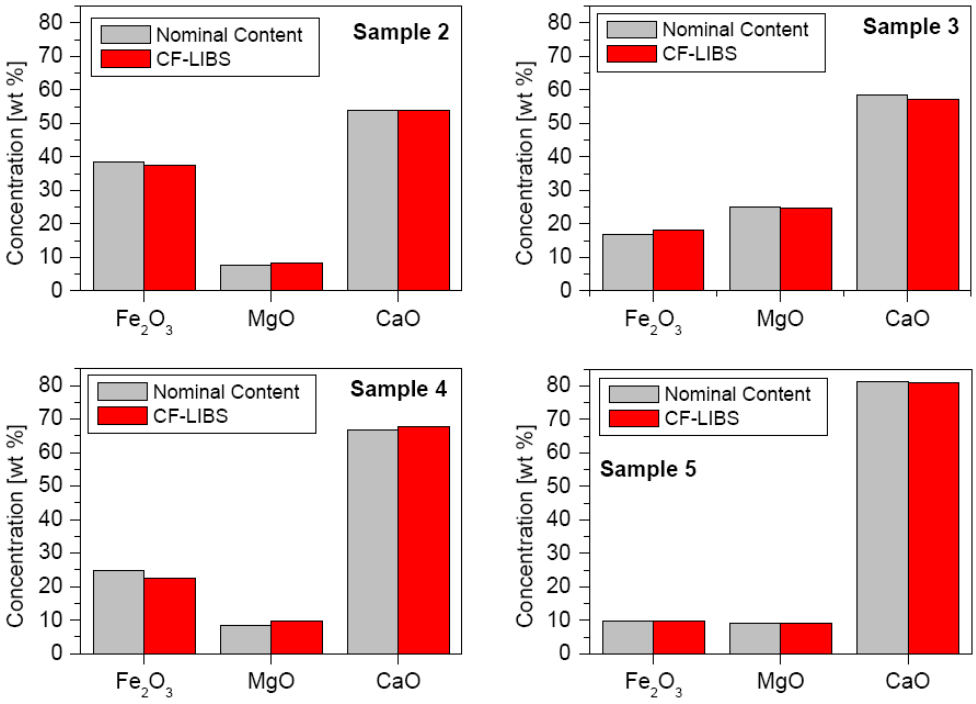

Figure 3. CF-LIBS analysis of four samples containing different amount of iron oxide, magnesium oxide, and calcium oxide. Oxide concentration as determined by CF-LIBS (red columns) and nominal concentration (grey columns).

Table 3. Relative and absolute errors in CF-LIBS analysis of mixed oxide materials.

		Fe_2O_3	**MgO**	**CaO**
Relative error	$e_r = \lvert C_{Nominal} - C_{CF-LIBS} \rvert / C_{Nominal}$	< 10 %	< 20 %	< 5 %
Absolute error	$e_a = \lvert C_{Nominal} - C_{CF-LIBS} \rvert$	< 2.5 wt %	< 1.5 wt %	< 1.1 wt %

Sample # 1 was used to test the convergence of the iterative algorithm. Results of CF-LIBS analysis of samples # 2-5 are summarized in Figure 3 and Table 3. The oxide concentration obtained from CF-LIBS analysis, $C_{CF\text{-}LIBS}$, and the nominal concentration, $C_{Nominal}$, are very close for all samples investigated. Table 3 shows the relative and absolute errors. The results indicate that CF-LIBS can be employed for quantitative analysis of major elements in multi-component materials.

4. CONCLUSIONS

Pulsed-laser deposition and laser-induced breakdown spectroscopy are powerful techniques for the synthesis and analysis of many different materials. PLD enables growing oxide thin films, heterostructures, and non-planar structures with a precision down to the atomic scale. The up-scaling of this technique for high through-put production of coated tapes has been demonstrated by several groups. LIBS is a spectro-chemical technique that is used for fast analysis of materials without sample preparation. The application fields of LIBS are manifold including homeland security, environmental sensing, materials identification, sorting, cultural heritage, and process control. Both techniques, PLD and LIBS, have developed rapidly in the past years. New sources of radiation and advanced instrumentation will support this development and lead to new applications of lasers in materials synthesis and spectroscopic analysis.

ACKNOWLEDGEMENTS

Several colleagues at the Johannes Kepler University Linz contributed to the work presented here. I am grateful to Dieter Bäuerle for stimulating discussions and to Johannes Heitz for the intense co-operation on LIBS. Marius A. Bodea and Khurram Siraj prepared YBCO films by PLD and contributed to ion-beam nano-patterning of films. Bernhard Praher developed the refined CF-LIBS algorithm and tested it using mixed-oxide samples. The industrial partners of the Christian Doppler laboratory, voestalpine Stahl GmbH and AVE Österreich GmbH, provided valuable input. Financial support by the Austrian Federal Ministry of Economy, Family and Youth and the National Foundation for Research, Technology and Development (Christian Doppler Laboratory LAD), the Austrian Science Fund (FWF project P18320), and the European Science Foundation (ESF project “Nanoscience and Engineering in Superconductivity”) is gratefully acknowledged.

REFERENCES

[1] Bäuerle, D., [Laser Processing and Chemistry], 3rd edition, Springer (2000).
[2] Chrisey, D. B. and Hubler, G. K., [Pulsed Laser Deposition of Thin Films], John Wiley & Sons Inc (1994).
[3] Eason, R., (Ed.), [Pulsed Laser Deposition of Thin Films: Applications-Led Growth of Functional Materials], Wiley (2007).
[4] Cremers, D. A. and Radziemski, L. J., [Handbook of Laser-Induced Breakdown Spectroscopy], John Wiley & Sons Inc (2006).
[5] Miziolek, A. W., Palleschi, V. and Schechter I., (Eds.), [Laser-Induced Breakdown Spectroscopy (LIBS), Fundamentals and Applications], Cambridge University Press (2006).
[6] Singh, J. P. and Thakur, S. N., (Eds.), [Laser Induced Breakdown Spectroscopy], Elsevier (2007).
[7] Löbe, A., Vrenegor, J., Fleige, R., Sturm, V. and Noll, R., "Laser-induced ablation of a steel sample in different ambient gases by use of collinear multiple laser pulses", Analytical and Bioanalytical Chemistry 385, 326-332 (2006).
[8] Ferrero, A. and Laserna, J. J., "A theoretical study of atmospheric propagation of laser and return light for stand-off laser induced breakdown spectroscopy purposes", Spectrochimica Acta Part B 63, 305-311 (2008).
[9] Usoskin, A., Rutt, A., Freyhardt, H. C., Prause, B., Schlenga, K., Saugrain, J.-M., Allais, A. and Willén, D., "HTS Coated Conductors Developed for the European Super3C Cable", IEEE/CSC & ESAS EUROPEAN SUPERCONDUCTIVITY NEWS FORUM (ESNF), No. 10, page 1-8, October 2009.
[10] Fuji, H., Igarashi, M., Hanada, Y., Miura, T., Hanyu, S., Kakimoto, K., Iijima, Y. and Saitoh T., "Long Gd-123 coated conductor by PLD method", Physica C 468, 1510-1513 (2008).
[11] Ogale, S. B., (Ed.), [Thin Films and Heterostructures for Oxide Electronics], Springer (2005).

[12] Ohtomo, A. and Hwang, H. Y., "A high-mobility electron gas at the $LaAlO_3/SrTiO_3$ heterointerface", Nature 427, 423-426 (2004).
[13] Thiel, S., Hammerl, G., Schmehl, A., Schneider, C. W. and Mannhart, J., "Tunable Quasi–Two-Dimensional Electron Gases in Oxide Heterostructures", Science 313, 1942-1945 (2006).
[14] Dam, B., Huijbregtse, J. M., Klaassen, F. C., van der Geest, R. C. F., Doornbos, G., Rector, J. H., Testa, A. M., Freisem, S., Martinezk, J. C., Stäuble-Pümpin, B. and Griessen, R., "Origin of high critical currents in $YBa_2Cu_3O_{7-\delta}$ superconducting thin films", Nature 399, 439-442 (1999).
[15] Lee, H. N., Christen, H. M., Chisholm, M. F., Rouleau, C. M. and Lowndes, D. H., "Strong polarization enhancement in asymmetric three-component ferroelectric superlattices", Nature 433, 395-399 (2005).
[16] Cao, B. Q., Zúniga-Pérez, J., Boukos, N., Czekalla, C., Hilmer, H., Lenzner, J., Travlos, A., Lorenz, M. and Grundmann, M., "Homogeneous core/shell ZnO/ZnMgO quantum well heterostructures on vertical ZnO nanowires" Nanotechnology 20, 305701 (2009).
[17] Pedarnig, J. D., Rössler, R., Delamare, M. P., Lang, W., Bäuerle, D., Köhler, A. and Zandbergen, H.W., "Electrical properties, texture and microstructure of vicinal $YBa_2Cu_3O_{7-\delta}$ thin films", Applied Physics Letters 81(14), 2587-2589 (2002).
[18] Rössler, R., Pedarnig, J. D. and Jooss Ch., "$Bi_2Sr_2Ca_{n-1}Cu_2O_{2(n+2)+\delta}$ thin films on c – axis oriented and vicinal substrates", Physica C 361(1), 13-21 (2001).
[19] Yun, S. H., Pedarnig, J. D., Rössler, R., Bäuerle, D. and Obradors X., "In-plane and out-of-plane resistivities of vicinal Hg – 1212 thin films", Applied Physics Letters 77(9), 1369-1371 (2000).
[20] Galca, A. C., Secu, M., Vlad, A. and Pedarnig, J. D., "Optical properties of zinc oxide thin films doped with aluminum and lithium", Thin Solid Films 518, 4603-4606 (2010).
[21] Vlad, A., Yakunin, S., Kolmhofer, E., Kolotovska, V., Muresan, L., Sonnleitner, A., Bäuerle, D. and Pedarnig, J. D., "Deposition, characterization and biological application of epitaxial Li:ZnO / Al:ZnO double-layers", Thin Solid Films 518, 1350-1354 (2009).
[22] Epurescu, G., Vlad, A., Bodea, M. A., Vasiliu, C., Dumitrescu, O., Niciu, H., Elisa, M., Siraj, K., Pedarnig, J. D., Bäuerle, D., Filipescu, M., Nedelcea, A., Galca, A. C., Grigorescu, C. E. A. and Dinescu, M., "Pulsed-laser deposition of smooth thin films of Er, Pr and Nd doped glasses", Applied Surface Science 255, 5295-5298 (2009).
[23] Siraj, K., Pedarnig, J. D., Moser, A., Bäuerle, D., Hari Babu, N. and Cardwell, D. A., "Enhanced self-field critical current density of nano-composite $YBa_2Cu_3O_7$ thin films grown by pulsed-laser deposition", Europhysics Letters 82, 57006 (2008).
[24] Lang, W., Dineva, M., Marksteiner, M., Enzenhofer, T., Siraj, K., Peruzzi, M., Pedarnig, J. D., Bäuerle, D., Korntner, R., Cekan, E., Platzgummer, E. and Loeschner, H., "Ion-beam direct-structuring of high-temperature superconductors", Microelectronic Engineering 83, 1495-1498 (2006).
[25] Bodea, M. A., Pedarnig, J. D., Siraj, K., Behbood, N., Bäuerle, D., Lang, W., Hasenfuss, C., Palmetshofer, L., Haselgrübler, K., Kolarova, R. and Bauer P., "Modification and nano-patterning of high-T_c superconducting thin films by masked ion beam irradiation", Journal of Physics: Conference Series 234, 012005 (2010).
[26] Markowitsch, W., Steiger, B., Lang, W., Bodea, M. A. and Pedarnig, J. D., "Optically induced changes and long-term relaxations of resistivity and critical temperature in He^+ irradiated $YBa_2Cu_3O_x$", Thin Solid Films 518, 7070-7074 (2010).
[27] Pedarnig, J. D., Siraj, K., Bodea, M. A., Puica, I., Lang, W., Kolarova, R., Bauer, P., Haselgrübler, K., Hasenfuss, C., Beinik, I. and Teichert, C., "Surface planarization and masked ion-beam structuring of $YBa_2Cu_3O_7$ thin films", Thin Solid Films 518, 7075-7080 (2010).
[28] Noll, R., Sturm, V., Aydin, Ü., Eilers, D., Gehlen, C., Höhne, M., Lamott, A., Makowe, J. and Vrenegor, J., "Laser-induced breakdown spectroscopy - From research to industry, new frontiers for process control", Spectrochimica Acta Part B 63, 1159-1166 (2008).
[29] Cabalín, L. M., González, A., Ruiz, J. and Laserna, J. J., "Assessment of statistical uncertainty in the quantitative analysis of solid samples in motion using laser-induced breakdown spectroscopy", Spectrochimica Acta Part B 65, 680-687 (2010).
[30] Stehrer, T., Praher, B., Viskup, R., Jasik, J., Wolfmeir, H., Arenholz, E., Heitz, J. and Pedarnig, J. D., "Laser-induced breakdown spectroscopy of iron oxide powder", Journal of Analytical Atomic Spectrometry 24, 973-978 (2009).
[31] Pedarnig, J. D., Heitz, J., Stehrer, T., Praher, B., Viskup, R., Siraj, K., Moser, A., Vlad, A., Bodea, M. A., Bäuerle, D., Hari Babu, N. and Cardwell, D. A., "Characterization of nano-composite oxide ceramics and

monitoring of oxide thin film growth by laser-induced breakdown spectroscopy", Spectrochimica Acta Part B 63, 1117-1121 (2008).
[32] Ciucci, A., Corsi, M., Palleschi, V., Rastelli, S., Salvetti, A. and Tognoni, E., "New procedure for quantitative elemental analysis by Laser Induced Plasma Spectroscopy", Applied Spectrosccopy 53, 960–964 (1999).
[33] Praher, B., Palleschi, V., Viskup, R., Heitz, J. and Pedarnig, J. D., "Calibration free laser-induced breakdown spectroscopy of oxide materials", Spectrochimica Acta Part B 65, 671–679, (2010).